0026-895X/04/6602-276–284$20.00
MOLECULAR PHARMACOLOGY
Copyright © 2004 The American Society for Pharmacology and Experimental Therapeutics
Mol Pharmacol 66:276–284, 2004

Vol. 66, No. 2
1917/1163132
Printed in U.S.A.

The N-terminal Ca^{2+}-Independent Calmodulin-Binding Site on the Inositol 1,4,5-trisphosphate Receptor Is Responsible for Calmodulin Inhibition, Even Though This Inhibition Requires Ca^{2+}

Nael Nadif Kasri, Geert Bultynck, Jeremy Smyth, Karolina Szlufcik, Jan B. Parys, Geert Callewaert, Ludwig Missiaen, Rafael A. Fissore, Katsuhiko Mikoshiba, and Humbert de Smedt

Laboratorium voor Fysiologie, Katholieke Universiteit Leuven Campus Gasthuisberg O/N, Leuven, Belgium (N.N.K., G.B., K.S., J.B.P., G.C., L.M., H.d.S.); Molecular and Cellular Biology Program and Department of Veterinary and Animal Sciences, University of Massachusetts, Amherst, Massachusetts (J.S., R.A.F.); and Department of Molecular Neurobiology, Institute of Medical Science, University of Tokyo, Tokyo, Japan (K.M.)

Received February 25, 2004; accepted April 18, 2004

This article is available online at http://molpharm.aspetjournals.org

ABSTRACT

Calmodulin (CaM) is a ubiquitous Ca^{2+}-sensor protein that plays an important role in regulating a large number of Ca^{2+} channels, including the inositol 1,4,5-trisphosphate receptor (IP_3R). CaM binds to the IP_3R at Ca^{2+}-dependent as well as at Ca^{2+}-independent interaction sites. In this study, we have investigated the Ca^{2+}-independent CaM-binding site for its role in the regulation of the Ca^{2+}-dependent bell-shaped activation curve of the IP_3R. Suramin, a polysulfonated napthylurea, displaced CaM in both the presence and the absence of Ca^{2+}. Suramin competed with CaM for binding to different peptides representing the previously identified CaM-binding sites on IP_3R1. By interacting with the N-terminal Ca^{2+}-independent CaM-binding site, suramin mimicked the functional effect of CaM and induced an allosteric but competitive inhibition of IP_3 binding. Therefore, suramin also potently inhibited IP_3-induced Ca^{2+} release (IICR) from permeabilized cells predominantly expressing IP_3R1 (L15 fibroblasts) or IP_3R3 (Lvec fibroblasts), even though the IP_3R3 does not contain Ca^{2+}-dependent CaM-binding sites. Furthermore, we have found that CaM_{1234}, a CaM mutated in its four EF hands, inhibited IICR in a Ca^{2+}-dependent way with the same potency as CaM. We conclude that CaM inhibits IICR via the N-terminal binding site. The inhibition requires Ca^{2+} but CaM itself is not the Ca^{2+} sensor for the inhibition of the IP_3R.

Inositol 1,4,5 trisphosphate receptors (IP_3Rs) are ubiquitous intracellular Ca^{2+}-release channels that are regulated in a complex way by Ca^{2+}. Low Ca^{2+} concentrations ($[Ca^{2+}]$) stimulate IP_3R activity, whereas higher $[Ca^{2+}]$ inhibit IP_3R activity. The positive regulation of the IP_3R by Ca^{2+} may be largely attributable to a direct binding of Ca^{2+} to the receptor (Miyakawa et al., 2001). The mechanism by which Ca^{2+} inactivates IP_3Rs is less clear. One suggestion is that calmodulin (CaM) mediates the Ca^{2+}-dependent inactivation of IP_3Rs (Michikawa et al., 1999; Missiaen et al., 1999; Adkins et al., 2000). However, this hypothesis is controversial because mutation of a critical tryptophane residue in the most prominent high-affinity Ca^{2+}-dependent CaM-binding site (Yamada et al., 1995) largely eliminated Ca^{2+}-dependent CaM binding but did not prevent inactivation of IP_3Rs by Ca^{2+} (Zhang and Joseph, 2001; Nosyreva et al., 2002). Both Ca^{2+}-dependent and -independent CaM-binding sites have been mapped to different regions of the IP_3Rs (Nadif Kasri et al., 2002; Taylor and Laude, 2002). A Ca^{2+}-dependent CaM-binding site was identified in the regulatory domain, whereas a Ca^{2+}-independent CaM-binding site was found in the N-terminal part of the IP_3R (Nadif Kasri et al., 2002; Taylor

Work performed by the authors was supported by grants G.0210.03 (to H.D.S. and J.B.P.) and G.O206.01 (to L.M.) of the Fund for Scientific Research Flanders (Belgium), and by grant 99/08 from the Concerted Actions of the Katholieke Universiteit Leuven (to L.M., H.D.S., G.C., and J.B.P.). G.B. is a postdoctoral fellow of the Fund for Scientific Research Flanders (Belgium) and has a fellowship of the Belgian American Educational Foundation (B.A.E.F.). R.A.F. has a senior postdoctoral fellowship of the Fund for Scientific Research Flanders (Belgium). We are also grateful for the support by the Interuniversity Poles of Attraction Programme-Belgian State, Prime Minister's Office, Federal Office for Scientific, Technical, and Cultural Affairs, IUAP P5/05.

ABBREVIATIONS: IP_3R, inositol 1,4,5-trisphosphate receptor; IP_3, inositol 1,4,5-trisphosphate; CaM, calmodulin; $[Ca^{2+}]$, calcium concentration; RyR, ryanodine receptor; IICR, IP_3-induced Ca^{2+} release; aa, amino acid(s); apoCaM, apocalmodulin; dCaM, dansylated CaM; CaBP, calcium-binding protein; A23187, 4-bromocalcimycin.

and Laude, 2002). Ca^{2+}-independent CaM binding caused a significant decrease in the affinity of IP_3Rs for their ligand (Patel et al., 1997; Sipma et al., 1999; Adkins et al., 2000; Vanlingen et al., 2000; Sienaert et al., 2002). This interaction may provide a tonic regulation of IP_3R activity, and could explain the low sensitivity of IP_3-induced Ca^{2+} release (IICR) in neuronal tissues in which CaM is highly expressed (Khodakhah and Ogden, 1993). However, the precise mechanism of the regulation of IP_3Rs by CaM is unclear, because the functional effects of CaM, particularly the Ca^{2+} dependence of the inhibition, could not be correlated with the molecular data.

In this study, we have investigated the functional effects of CaM on the IP_3R, particularly the role of its N-terminal CaM-binding site. We have used suramin, a polysulfonated napthylurea, to investigate the molecular mechanism of the inhibition of the IP_3R by CaM. Suramin has been shown to interact in a direct way with different types of CaM-binding sites (Klinger et al., 2001). Suramin interacted directly with the CaM-binding sites of the ryanodine receptor (RyR) and thereby counteracted the effects of CaM (Papineni et al., 2002). We now report that suramin interacted with the different identified CaM-binding sites on the IP_3R in both the presence and the absence of Ca^{2+}. Suramin thereby strongly inhibited IICR. The functional importance of the N-terminal Ca^{2+}-independent CaM-binding site in this inhibition was confirmed by the finding that CaM_{1234}, a CaM mutant that is unable to bind Ca^{2+}, had the same inhibitory effect on the IP_3R as wild-type CaM. Moreover, other CaM-like Ca^{2+}-sensor proteins, such as calcium-binding protein 1 (CaBP1), which was recently shown to strongly inhibit IICR and to interact at the same N-terminal site of the IP_3R (Haynes et al., 2004; Nadif Kasri et al., 2004) inhibited IICR by a mechanism similar to that of CaM. We conclude that suramin and CaM are inhibitors of IP_3 binding by allosteric binding to an N-terminal Ca^{2+}-independent site. The same interaction is also responsible for inhibition of IICR, but IICR inhibition only occurs in the presence of Ca^{2+}. CaM, however, is not the Ca^{2+} sensor for this inhibition.

Materials and Methods

Materials. Suramin was purchased from Sigma Aldrich (Belgium). All other biochemicals were of the highest quality available.

Construction of Plasmids. For the construction of pGEX6p2 vector (Amersham Biosciences, Uppsala, Sweden) encoding aa 1 to 225 of mouse IP_3R1, the coding region was amplified from the pcDNA3.1(+)-mouse IP_3R1 as a template by a PCR reaction with forward-primer 5′-TAACCGGATCCATGTCTGACAAAATGTCGAG-3′ and reverse primer 5′-CTCCCGAATTCTCATTTCATGAAAAGCACTATCTTC-3′. The PCR product was digested with BamHI and EcoRI (respective restriction sites are underlined) and cloned into the BamHI/EcoRI-treated pGEX6p2 vector. Constructs were sequenced using the Automated Fluorescent sequencing system (Amersham Biosciences).

Expression of IP_3R. Expression of wild-type IP_3R1 in Sf9 cells using the baculovirus expression system was described previously (Sipma et al., 1999). Wild-type IP_3R1 was permanently expressed in R23–11 triple-IP_3R knockout cells (Sugawara et al., 1997) by electroporation and subsequent selection on 1.2 mg/ml G418 (Geneticin; Invitrogen, Carlsbad, CA) (Miyakawa et al., 1999).

Preparation of Microsomes. Total Sf9 microsomes were prepared as described previously (Yoneshima et al., 1997). R23-11 suspension cells were harvested by centrifugation for 5 min at 4000*g* and washed twice with phosphate-buffered saline without Ca^{2+} and Mg^{2+}. Cell pellets were resuspended in homogenization buffer (10 mM Tris-HCl, pH 7.4, 1 mM EGTA, 0.8 mM benzamidine, 0.2 mM phenylmethylsulfonyl fluoride, 0.5 μg/ml leupeptin, 0.5 μg/ml aprotinin, and 0.5 μg/ml pepstatin A) and homogenized on ice with a probe sonicator (three times 20 s) (MSE Ltd., Crawley, Surrey, UK). Total microsomes were obtained by centrifugation for 25 min at 125,000*g*. The membranes were resuspended in isotonic medium (20 mM Tris-HCl, pH 7.4, 300 mM sucrose, 0.8 mM benzamidine, and 0.2 mM phenylmethylsulfonyl fluoride). Microsomal preparations were stored at −80°C.

Purification of GST-Fusion Proteins. For preparation of GST-fusion proteins, pGEX6p2 vector containing the coding sequence for aa 1 to 225 N-terminal of mouse IP_3R1 was transformed into BL21(DE3) *Escherichia coli*. Colonies were grown overnight in 50 ml of Luria-Bertani medium at 37°C. Luria-Bertani medium (400 ml) was added to this preculture, and bacteria were further grown at 37°C until A_{600} amounted to 0.8. Protein expression was induced by adding 0.1 mM isopropyl-thio-β-D-galactopyranoside to the bacterial culture, which was further grown at 24°C for another 3 h. Bacterial cells were harvested and lysed by sonication. The soluble fraction was incubated for 2 h with glutathione-Sepharose 4B beads (Amersham Biosciences). After washing the beads, immobilized GST-fusion protein was treated for 2 h at 4°C with PreScission Protease (40 U) (Amersham Biosciences) in cleavage buffer (50 mM Tris-HCl, pH 7.0, 150 mM NaCl, 1 mM EDTA, and 1 mM 1,1,1-trichloro-2,2-bis-(4′-chlorophenyl)ethane). After centrifugation of the beads, purified 1 to 225 protein was recovered in the supernatant. Purified protein was dialyzed overnight against phosphate-buffered saline, using Slide-A-Lyzer with a cut-off of 10 kDa (Pierce Biotechnology Inc., Rockford, IL) and stored at −80°C.

Expression and Purification of Recombinant Proteins. CaM, CaM_{1234}, and CaBP1 were expressed and purified as described previously (Nadif Kasri et al., 2003).

CaM-Sepharose Pull-Down Assay. CaM-Sepharose 4B (50 μl; Amersham Biosciences) or Sepharose 4B (control) was incubated with 500 ng of purified IP_3R (Maes et al., 2001) or 10 μg of purified bacterial protein (N-terminal aa 1 to 225 of IP_3R1) for 2 h at 4°C in incubation buffer [i.e., one part Tris-buffered saline (20 mM Tris-HCl, pH 7.2, and 150 mM NaCl) mixed with one part bacterial lysis buffer (Pierce), supplemented with 1 mM β-mercaptoethanol]. Unbound protein was removed by washing the Sepharose beads four times with 500 μl of the incubation buffer. Bound IP_3R1 or 1 to 225 protein was eluted by incubating the beads with LDS (Invitrogen) for 10 min at 70°C, and the beads were removed by centrifugation at 20,000*g* for 1 min. All samples were separated on NuPAGE® 4–12% Bis-Tris SDS-PAGE gels and analyzed by Western blotting, using a polyclonal antibody directed against a conserved N-terminal region (aa 127–141) of the IP_3R [Rbt475 (1/2500)] as the primary antibody.

Nondenaturing Gel Electrophoresis. The electrophoretic mobility of CaM was evaluated by nondenaturing discontinuous PAGE as described by Laemmli (1970). Nondenaturing gels were run at 25 mA and 4°C under high Ca^{2+} conditions (200 μM free Ca^{2+} in all gel buffers) or low Ca^{2+} conditions (1 mM EGTA in all gel buffers). Quantification of the intensity of the CaM bands was done by Imagequant 4.2 (volume quantitation analyses of the pixel intensities within selected objects; Amersham Biosciences).

[^{3}H]IP_3 Binding. Binding studies were performed as described previously (Sipma et al., 1999). [^{3}H]IP_3 binding was performed at 0°C in 100 μl of binding buffer containing 50 mM Tris/HCl, pH 7.0, 1 mM EGTA, and 10 mM β-mercaptoethanol. After 30 min of incubation, 10 μl of γ-globulin (20 mg/ml) and 110 μl of 20% (w/v) polyethylene glycol in IP_3-binding solution were added, and the samples were rapidly filtered through glass-fiber filters. The amount of purified protein used ranged between 2.5 and 8 μg. Nonspecific binding was determined in the presence of 12.5 μM unlabeled IP_3. Statistical analysis was performed using the paired Student's *t* test. Values were considered significantly different when $P < 0.01$.

$^{45}Ca^{2+}$ Fluxes. $^{45}Ca^{2+}$ fluxes were performed on saponin-permeabilized Lvec and L15 cells (Miyawaki et al., 1990; Mackrill et al., 1996) in essentially the same way as described previously for A7r5 cells (Missiaen et al., 1999). L15 cells were obtained by stable exogenous expression of IP_3R1 in L cells, whereas Lvec cells represent the control cells expressing the empty plasmid vector (Miyawaki et al., 1990; Mackrill et al., 1996). The cells were seeded in 12-well clusters (Costar, MA) at a density of approximately 4×10^4 cm^{-2}. Experiments were carried out on confluent monolayers of cells (3×10^5 cells/well) between the 7th and 9th day after plating. Cells were permeabilized by incubating them for 10 min with a solution containing 120 mM KCl, 30 mM imidazole-HCl, pH 6.8, 2 mM $MgCl_2$, 1 mM ATP, 1 mM EGTA, and 20 μg/ml saponin at 25°C. The nonmitochondrial Ca^{2+} stores were loaded for 45 min at 25°C in 120 mM KCl, 30 mM imidazole-HCl, pH 6.8, 5 mM $MgCl_2$, 5 mM ATP, 0.44 mM EGTA, 10 mM NaN_3, and 150 nM free $^{45}Ca^{2+}$ (23 μCi/ml). The cells were then washed twice with 1 ml of efflux medium containing 120 mM KCl, 30 mM imidazole-HCl, pH 6.8, 1 mM EGTA, and 10 μM thapsigargin. Thapsigargin was added to block the endoplasmic reticulum Ca^{2+} pumps. The efflux medium was replaced every 2 min for 18 min, and the efflux was performed at 25°C. Free [Ca^{2+}] was calculated by the Cabuf program (ftp://ftp.cc.kuleuven.ac.be/pub/droogmans/cabuf.zip) and based on the stability constants given by Fabiato and Fabiato (1979). At the end of the experiment, the $^{45}Ca^{2+}$ remaining in the stores was released by incubation with 1 ml of a 2% SDS solution for 30 min. Ca^{2+} release is plotted as the fractional loss (i.e., the amount of Ca^{2+} released in 2 min divided by the total store Ca^{2+} content at that time). The latter value was calculated by summing in retrograde order the amount of tracer remaining in the cells at the end of the efflux and the amounts of tracer collected during the successive time intervals. The Ca^{2+} release was normalized to the total releasable fraction by 5 μM A23187, which was taken as 100%.

Results

Suramin Interacts with the CaM-Binding Sites on the IP_3R. Three CaM-binding sites have been described on the IP_3R1: a low-affinity site near the N terminus of the IP_3R1 that essentially binds CaM in a Ca^{2+}-independent way (Adkins et al., 2000; Sienaert et al., 2002); a high-affinity site in the regulatory domain that mainly binds Ca^{2+}/CaM (Yamada et al., 1995); and a third site that only appears after splicing out of S2 (i.e., in peripheral tissues) (Islam et al., 1996; Lin et al., 2000). To determine whether suramin interacts with the CaM-binding sites on the IP_3R1, purified IP_3R1 was pulled down on a CaM-Sepharose column. Figure 1A shows the interaction of CaM with IP_3R1 both in EGTA and in the presence of 200 μM Ca^{2+}. The IP_3R binding on the CaM-Sepharose column seemed to be largely Ca^{2+}-dependent. This is also compatible with previous findings that a single mutation (W1576A) largely abolished the Ca^{2+} dependent binding to the CaM-Sepharose column (Yamada et al., 1995). We observed, however, that there remained a lower but significant CaM binding in the absence of Ca^{2+} (Fig. 1A, lane 3). This could be a result of either a contribution from the N-terminal CaM-binding site or a partially Ca^{2+}-independent interaction with the CaM-binding site in the regulatory domain. The presence of 1 μM suramin during the binding reaction completely abolished the interaction of CaM with the IP_3R1. This inhibition was observed for the interaction in the presence of Ca^{2+} as well as for the much weaker interaction in the absence of Ca^{2+} (Fig. 1A).

To investigate the interaction of suramin with the N-terminal CaM-binding site, we performed pull-down experiments of the recombinant 1 to 225 N-terminal domain on a CaM-Sepharose column. The aa 1 to 225 protein was recombinantly expressed in bacteria. This construct contained the low-affinity CaM-bin ding sites (aa 49–81 and aa 106–128) described previously (Sienaert et al., 2002). Figure 1B shows the interaction of the aa 1 to 225 protein with the CaM-Sepharose column. Suramin suppressed binding to the CaM-Sepharose column in the presence and absence of Ca^{2+}. Our results indicate that suramin interacts with the N-terminal CaM-binding site as well as with the CaM-binding site in the regulatory domain.

Suramin Binds to CaM-Binding Peptides of IP_3R1. To map the interaction site of suramin more precisely, we examined the ability of suramin to interact with synthetic peptides representing the CaM-binding domains of the IP_3R1 at both high and low [Ca^{2+}].

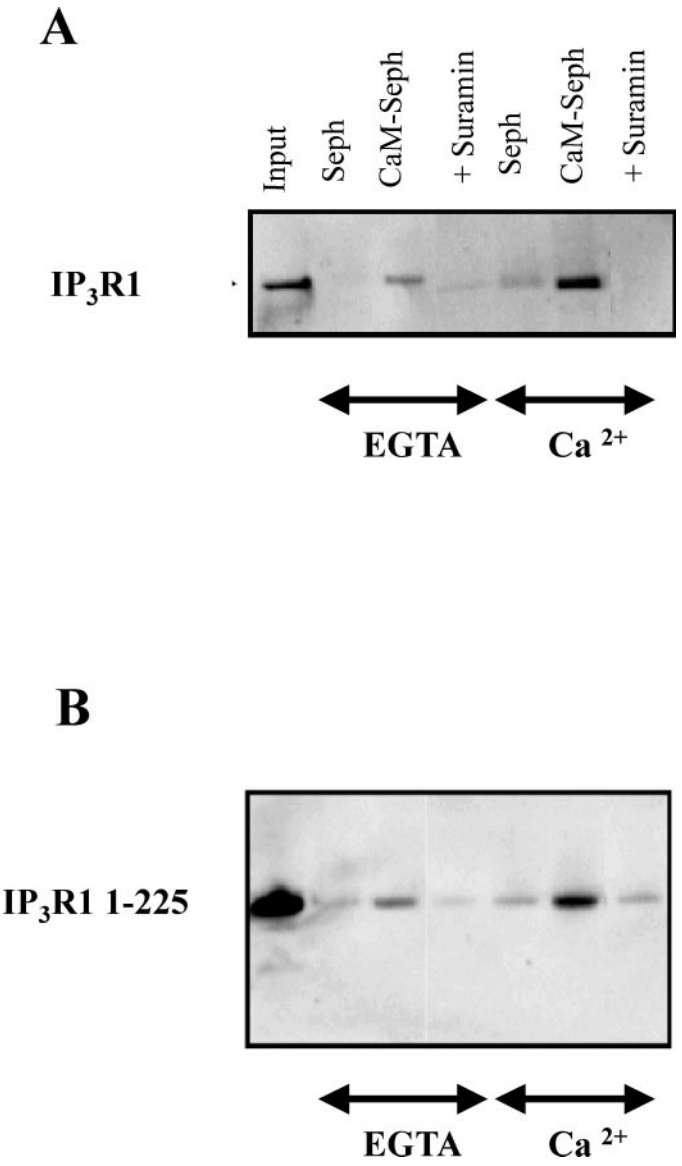

Fig. 1. Effect of suramin on the interaction of CaM with the IP_3R1. A, immunoblot showing the effects of 1 μM suramin on the interaction of full-size IP_3R1 from Sf9 cells with CaM-Sepharose in the absence (1 mM EGTA) and presence of Ca^{2+} (200 μM Ca^{2+}). B, immunoblot showing the effects of 1 μM suramin on the interaction of recombinantly expressed N-terminal aa 1 to 225 of IP_3R1 with CaM in the absence (1 mM EGTA) and presence of Ca^{2+} (200 μM Ca^{2+}).

Using band-shift assays, we have shown previously that CaM interacted with two peptides representing positions in the N terminus of IP_3R1: P49–81 and P106–128 (Sienaert et al., 2002). The interaction was Ca^{2+}-independent in that it occurred in both the absence and the presence of Ca^{2+}. A representative nondenaturing gel illustrating the interaction of the two peptides with CaM is shown in Fig. 2, A and B. The peptide-CaM complexes migrated as higher molecular weight bands than CaM, whereas the peptides alone do not enter the gel because they are positively charged. However, increasing the suramin concentrations disrupted the interaction between CaM and the peptides. This could be observed by the reappearance of the CaM band as a function of added suramin concentration (Fig. 2, A and B). Quantification of the intensity of the CaM bands in the presence of increasing concentrations of suramin in EGTA or in 200 μM free Ca^{2+} is shown in Fig. 2, C and D. For both peptides and in both conditions (EGTA or Ca^{2+}), suramin reversed the interaction with CaM.

It was originally shown that CaM interacted with aa 1564–1585 in the regulatory domain of IP_3R1 in a Ca^{2+}-dependent way (Yamada et al., 1995). Recent data suggested that apoCaM also binds to this region of the IP_3R1 (Adkins et al., 2000). One explanation for this finding is that both forms of CaM bind to closely located or overlapping sites within this region. To test this possibility, we synthesized a series of peptides (Fig. 3A) matching sequences around the cytosolic "1564–1585" site. We extended the peptides N- and C-terminal of the 1564–1585 region. The peptides all contained some similarity with known CaM-binding motifs [IQ or Baa motifs (Rhoads and Friedberg, 1997; Jurado et al., 1999)] (Fig. 3A, Table 1). A representative nondenaturing gel of CaM in the presence of four different peptides in either 200 μM free Ca^{2+} (Fig. 3B) or 1 mM EGTA (Fig. 3C) is shown. In Ca^{2+}-containing medium, CaM bound to peptides P1554–1585, P1564–1585, and P1564–1595, whereas in 1 mM EGTA, CaM bound only to P1554–1585. Densitometric analysis of CaM (1.5 μM) bands by ImageQuant 4.2 in the presence of 30 μM peptide is summarized for three independent experiments in Fig. 3D. These band-shift data were also confirmed by measuring fluorescence changes of dansylated CaM (dCaM). dCaM binding to a CaM-binding peptide is known to induce an increase in the emission spectrum of the dansyl moiety. We observed

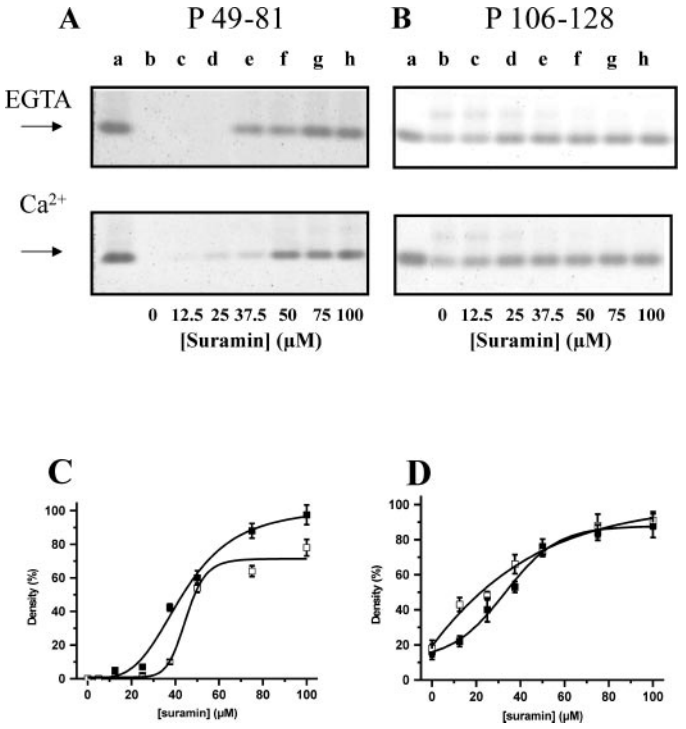

Fig. 2. The ability of suramin to inhibit CaM binding to the N-terminal CaM-binding site of IP_3R1. The effects of suramin on the interaction between CaM and IP_3R1 P49–81 (A) and P106–128 (B) were assessed by nondenaturing gel electrophoresis. Peptides (30 μM) and CaM (1.5 μM) were incubated in the absence (1 mM EGTA, top) or in the presence of Ca^{2+} (200 μM free Ca^{2+}, bottom) and in the presence of increasing concentrations of suramin, followed by electrophoresis and Sypro Orange staining. A and B, the arrow indicates the uncomplexed CaM band. Lane a, CaM alone; lane b, no suramin; lane c, 12.5 μM suramin; lane d, 25 μM suramin; lane e, 37.5 μM suramin; lane f, 50 μM suramin; lane g, 75 μM suramin; lane h, 100 μM suramin. C and D, densitometric analysis of uncomplexed CaM band in the presence of P49–81 (C) or P106–128 (D) and increasing concentrations of suramin, in the absence (■) or presence of Ca^{2+} (□).

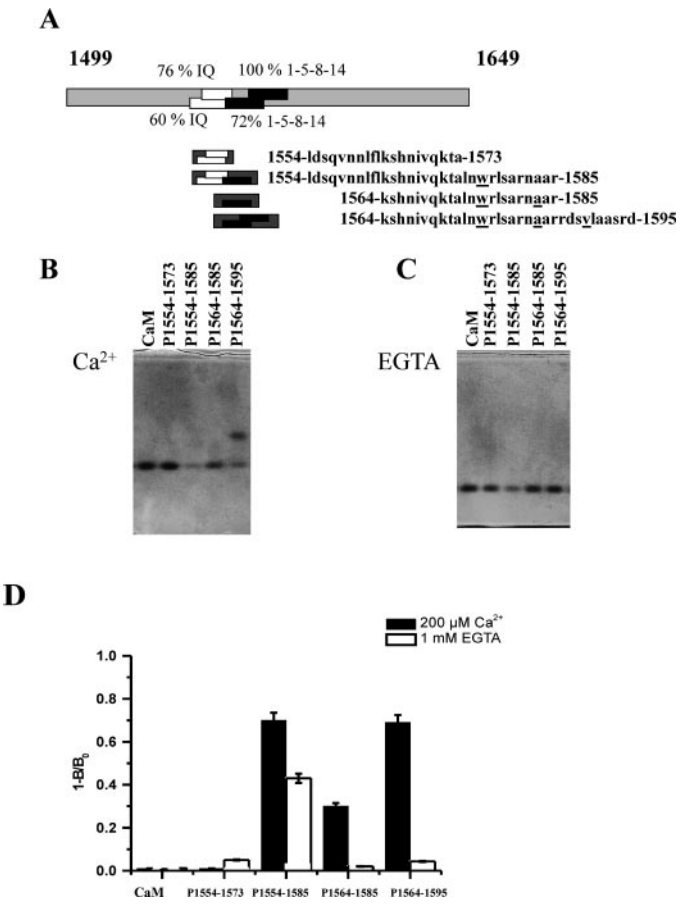

Fig. 3. Detailed analysis of the CaM-binding site in the regulatory domain of IP_3R1. A, schematic representation of the peptides used for the band-shift experiments. Known CaM-binding motifs are indicated. White bars represent IQ domains, and black bars represent Baa motifs. B and C, representative 15% nondenaturing gel of 1.5 μM CaM in the presence of each of the IP_3R1 peptides (30 μM): in a 50 mM Tris buffer, pH 7.4, containing either 200 μM free Ca^{2+} (B) or 1 mM EGTA (C) stained with Sypro Orange; the first lane represents the CaM input. Binding to CaM resulted in complexes with those peptides that did not enter the gel and therefore diminished the intensity of the CaM band, because of the formation of CaM-peptide complexes. D, densitometric analysis of the uncomplexed CaM band in the presence of the IP_3R1 peptides. The vertical axis denotes the intensity loss of the CaM bands after interaction with the peptides compared with the value for CaM in the absence of peptide.

these spectral changes when P1554–1585, P1564–1585, or P1564–1595 was added to a buffer containing dCaM (40 nM) in the presence of Ca^{2+}. In the absence of Ca^{2+}, spectral changes were observed only when P1554–1585 was added (data not shown). The apparent affinities of CaM binding to the peptides are shown in Table 1. In the presence of Ca^{2+} P1564–1595 shows the highest affinity (K_d, 64 ± 5 nM), whereas in the absence of Ca^{2+}, P1554–1585 was the only peptide that bound to CaM. P1554–1573 did not bind CaM in either of the two assays.

The results of the band-shift assays and dCaM assays indicate that the total region investigated here (aa 1554–1595) contains sites with affinities for both Ca^{2+}/CaM (K_d, 308 ± 18 nM) and apoCaM (K_d, 508 ± 24 nM). The previously determined boundaries of the cytosolic Ca^{2+}/CaM-binding site (Yamada et al., 1995), here represented by P1564–1585, therefore did not contain the apoCaM-binding site.

The effect of increasing concentrations of suramin on the interaction between CaM and P1554–1585 is shown in a representative nondenaturing gel of CaM (Fig. 4A). A densitometric analysis of this interaction is presented in Fig. 4B, showing that suramin interacted directly with P1554–1585 both in the presence and in the absence of Ca^{2+}. These data indicate that suramin interferes with all known CaM-binding sites on the IP_3R.

Suramin Inhibits IICR. We assessed the ability of suramin to act as a competitive antagonist to Ca^{2+}/CaM and apoCaM modulation of IP_3R1. Ca^{2+}/CaM was found to inhibit IP_3R channel activity and was proposed to be the Ca^{2+} sensor that confers Ca^{2+} inhibition of IP_3R channel activity (Michikawa et al., 1999). We reasoned, therefore, that suramin, by competing for endogenously bound CaM to the IP_3R1, could counteract the effects of CaM, as was demonstrated for the RyR (Papineni et al., 2002). IP_3-induced Ca^{2+} release (IICR) was measured in the presence and absence of suramin in permeabilized L15 and Lvec cells. Western blots indicated a 3/1 ratio for IP_3R1/IP_3R3 for L15 and the reverse ratio for Lvec cells (data not shown). This comparison was made because one major difference between both IP_3R isoforms is that IP_3R3 lacks the Ca^{2+}/CaM-binding site in the regulatory domain (Yamada et al., 1995).

In permeabilized L15 or Lvec cells, the addition of IP_3 to the efflux medium induced Ca^{2+} release from the nonmitochondrial internal stores. When suramin was added together with IP_3, IICR was inhibited in a concentration-dependent way. This inhibition occurred to the same extent in both cell lines. Dose response curves for suramin inhibition are presented in Fig. 5A. With 200 nM IP_3 in L15 cells or 1 μM IP_3 in Lvec cells, suramin half-maximally inhibited IICR at a concentration of 30 μM. This concentration is similar to that used for interaction with the CaM-binding site on the RyR (Papineni et al., 2002). For both cell lines, suramin decreased the apparent IP_3 sensitivity (Fig. 5B). In L15 cells and Lvec cells, 100 μM suramin increased the EC_{50} for IICR from 180 ± 16 nM to 1.09 ± 0.03 μM and from 890 ± 27 nM to 2.1 ± 0.04 μM, respectively. Furthermore, suramin had the same potency at different [Ca^{2+}]. This means that the bell-shaped regulation of the IP_3R was maintained (Fig. 5C).

Because suramin was previously shown to interfere with ATP-binding sites of the RyR (Emmick et al., 1994), we also investigated the possibility that suramin might inhibit IICR by interacting with the ATP-binding sites on the IP_3R. Therefore, IICR was measured in permeabilized L15 cells in the presence or absence of 1 mM ATP. As described previously, 1 mM ATP stimulated IICR (Maes et al., 2000, 2001). Suramin however inhibited IICR with the same potency under both conditions, suggesting that its effect was not caused by an interaction with the ATP-binding sites on the IP_3R1 (Fig. 6).

Suramin Inhibits IP_3 Binding. Because the inhibition by suramin was observed in cells predominantly expressing either IP_3R1 or IP_3R3, we investigated further the possibility that the CaM-binding site in the N-terminal part of the receptor, which is conserved among all isoforms (Vanlingen et al., 2000; Sienaert et al., 2002), could be responsible for this inhibition. CaM was previously shown to strongly inhibit IP_3 binding in a Ca^{2+}-independent way (Patel et al., 1997; Sipma et al., 1999; Vanlingen et al., 2000; Sienaert et al., 2002). IP_3 binding was measured on a recombinantly expressed protein containing the N-terminal aa 1 to 581 of IP_3R1 (Lbs1). Suramin (10 μM) inhibited IP_3 binding to Lbs1 by 42 ± 6% (Fig. 7A). Furthermore, we have used a deletion mutant Lbs1 Δ1–225, lacking the N-terminal aa 1 to 225. Lbs1 Δ1–225 was previously shown to bind IP_3 but to completely lack the CaM dependence (Sienaert et al., 2002). Similar to the CaM effects, the effect of suramin was totally abolished on Lbs1 Δ1–225 (Fig. 7A). These data suggest that the inhibition of IP_3 binding by suramin is caused by an allosteric interaction with the N-terminal CaM-binding sites. Scatchard analysis performed in the absence or presence of suramin (10 μM) yielded K_d values of 17 ± 3 nM and 55 ± 4 nM, respectively, whereas B_{max} values were not significantly different (481 ± 19 and 472 ± 23 pmol/mg; Fig. 7B). This indicates that suramin reduced the affinity of the IP_3-binding site but did not affect the number of IP_3-binding sites. Essentially the same results were obtained for microsomes of R23–11 cells expressing full-size IP_3R1 (data not shown).

CaM_{1234} Inhibits IICR. The inhibitory effects of CaM on IICR were observed only in the presence of Ca^{2+} (Adkins et

TABLE 1

Detailed analysis of the CaM-binding site in the regulatory domain of IP_3R1

Four different peptides were used in band-shift and dCaM assays to analyze the CaM-binding site in the regulatory domain. Peptide P1554–1585 was the only peptide found to bind in a Ca^{2+}-independent manner. P1564–1595 was found to have the highest affinity for Ca^{2+}/CaM.

Position	Motif	K_d, dCaM		Band-shift, CaM	
		Ca^{2+}	EGTA	Ca^{2+}	EGTA
		nM	*nM*		
L1554A1573	60% IQ-Motif	–	–	–	–
L1554R1585	60% IQ-Motif	308 ± 18	508 ± 24	++	++
K1564R1585	72% 1–5–8–14 Motif	104 ± 7	–	+	–
K1564R1595	100% 1–8–14 Motif	64 ± 5	–	++	–

+, interaction between peptide and CaM; –, no interaction between peptide and CaM.

al., 2000; Michikawa et al., 1999; Missiaen et al., 1999). These data therefore suggested that the Ca^{2+}-dependent CaM-binding site in the regulatory domain was responsible for this effect and that CaM could be the Ca^{2+} sensor for the IP_3R. However, mutational studies have clearly shown that mutation of this Ca^{2+}-dependent CaM-binding site does not alter the inhibition of IICR by Ca^{2+} (Zhang and Joseph, 2001; Nosyreva et al., 2002). Together with the fact that the CaM-binding site in the regulatory domain is not conserved among all isoforms, these results rather suggest a role for the Ca^{2+}-independent CaM-binding site in the N terminus. To clarify the molecular mechanism of the inhibition by CaM, we used CaM_{1234}, a mutant CaM that is unable to bind Ca^{2+}. We measured IICR in a $^{45}Ca^{2+}$-flux assay at different free [Ca^{2+}] (Fig. 8). In permeabilized L15 cells, the addition of 200 nM IP_3 to the efflux medium induced a Ca^{2+} release from non-mitochondrial internal stores. When 10 μM CaM or CaM_{1234} was added during the efflux, a similar inhibition in IICR was observed. Not only did CaM_{1234} have the same potency as CaM, but both forms of CaM were only effective at a minimum free [Ca^{2+}] of 300 nM (Fig. 8). Recently, evidence was provided that CaBP1, a member of the neuronal Ca^{2+}-sensor family, interacted with the N-terminal CaM-binding site of the IP_3R and mimicked the functional effects of CaM. Adding 10 μM CaBP1 during the efflux resulted in a Ca^{2+}-dependent inhibition of IICR very similar to that found for CaM and CaM_{1234} (Fig. 8). The same results were also observed with Lvec cells (data not shown). The inhibition by CaM_{1234} clearly shows that CaM does not act as the Ca^{2+} sensor for the inhibition of the IP_3R and that the inhibition of IICR is mediated by the N-terminal Ca^{2+}-independent CaM-binding site.

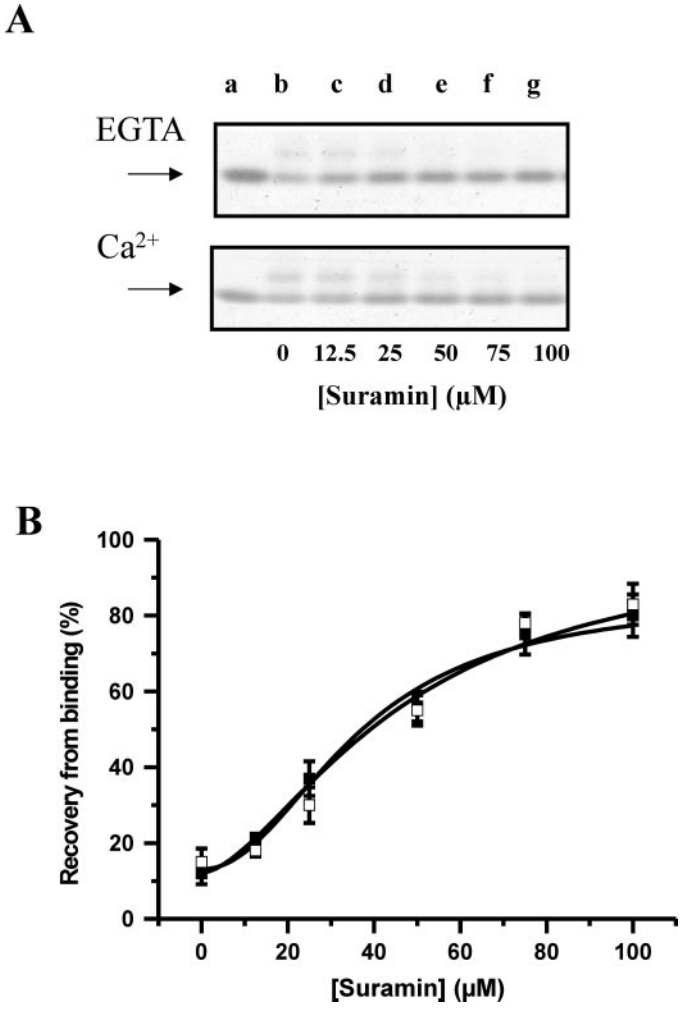

Fig. 4. The ability of suramin to inhibit CaM binding to the CaM-binding site of IP_3R1 in the regulatory domain. A, representative 15% nondenaturing gel of 1.5 μM CaM in the presence of the IP_3R1 P1554–1585 (30 μM) and increasing concentrations of suramin in a 50 mM Tris buffer, pH 7.4, containing either 1 mM EGTA (top) or 200 μM free Ca^{2+} (bottom) stained with Sypro Orange. Lane a, CaM input; lane b, no suramin; lane c, 12.5 μM suramin; lane d, 25 μM suramin; lane e, 50 μM suramin; lane f, 75 μM suramin; lane g, 100 μM suramin. B, densitometric analysis of uncomplexed CaM band in the presence of P1554–1585 and increasing concentrations of suramin in the absence (■) or presence of Ca^{2+} (□).

Discussion

Suramin is a polysulfonated napthylurea, which was reported to counteract CaM effects by binding to the CaM-binding sites of the RyR (Papineni et al., 2002). Our results

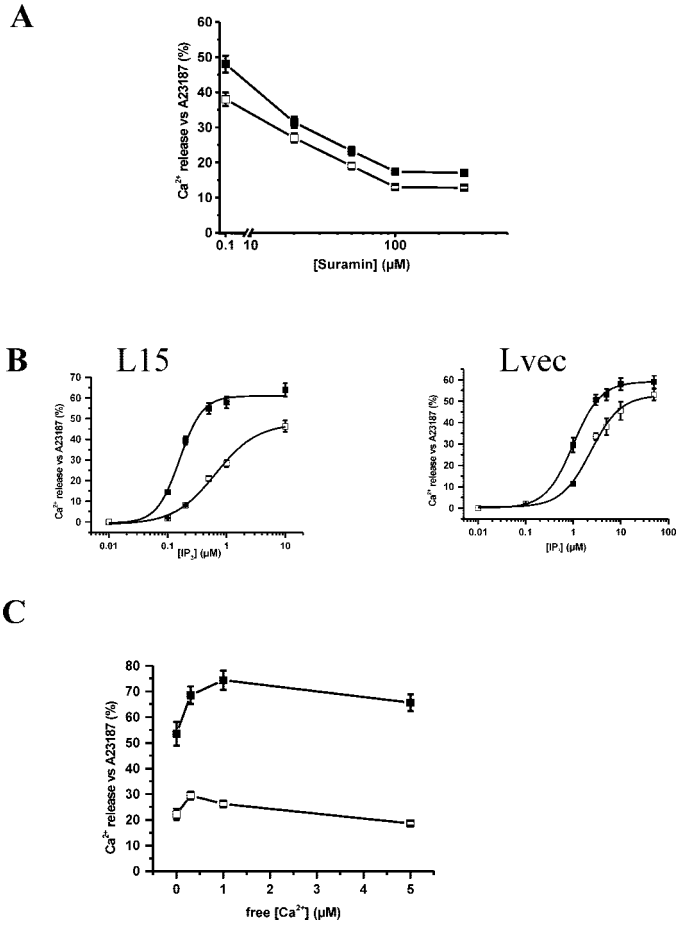

Fig. 5. Effect of suramin on IICR. A, Ca^{2+} release from permeabilized cells, loaded with $^{45}Ca^{2+}$ during 45 min, was measured after stimulation with 200 nM (L15 cells, ■) or 1 μM (Lvec, □) IP_3. Ca^{2+} release was plotted as a function of increasing concentration of suramin. B, Ca^{2+} release in L15 and Lvec cells was measured as a function of IP_3 in the absence (■) or presence (□) of 100 μM suramin. C, Ca^{2+} release from permeabilized L15 cells, loaded with $^{45}Ca^{2+}$ during 45 min, was measured after inducing the cells with 200 nM IP_3 at different free [Ca^{2+}] in the presence (□) or absence (■) of 100 μM suramin. Ca^{2+} release was always plotted as the percentage of the maximal releasable fraction by 5 μM A23187. Results represent the means ± S.E. of three independent experiments each performed twice.

indicate that suramin interacts in a competitive manner with all previously identified CaM-binding sites on the IP_3R. This interaction was seen in the presence and the absence of Ca^{2+} (Figs. 2 and 4).

We expected that suramin would counteract the effects of CaM and thereby stimulate IICR, as was previously demonstrated for the RyR. Surprisingly, however, suramin inhibited IICR in $^{45}Ca^{2+}$ flux assays (Fig. 5). As suramin inhibited IICR for IP_3R1 as well as for IP_3R3, we reasoned that the functional effects of suramin could be caused by its interaction with the conserved N-terminal CaM-binding domain. The absence of the suramin effects on IP_3 binding to a mutant lacking the N-terminal CaM-binding sites (Δ1–225) clearly showed that suramin allosterically inhibited IP_3 binding (Fig. 7). Effects on IICR can therefore be explained as a decrease in the apparent IP_3 affinity.

These data are at variance with previous models regarding the regulation of the IP_3R by CaM. It has been proposed that CaM is responsible for the Ca^{2+}-dependent inactivation of the IP_3R. The only known Ca^{2+}-dependent CaM-binding site, however, is not conserved in all three isoforms. Moreover, two studies have shown that mutation of the high-affinity CaM-binding site in the regulatory domain altered neither the Ca^{2+} dependence of the IP_3R nor the effects of CaM (Zhang and Joseph, 2001; Nosyreva et al., 2002). Based on the latter findings, it has been suggested that the N-terminal Ca^{2+}-independent CaM-binding site could be responsible for inhibition of IICR that was observed for the three isoforms (Adkins et al., 2000; Zhang and Joseph, 2001; Nosyreva et al., 2002). However, the Ca^{2+}-dependent effect of CaM could not be correlated with the Ca^{2+}-independent binding of CaM to that site. Therefore, we have used CaM_{1234}, a mutant CaM that is unable to bind Ca^{2+}. CaM_{1234} inhibited IICR in a Ca^{2+}-dependent way with the same potency as CaM. At low $[Ca^{2+}]$, CaM_{1234} had no effect on IICR; at higher $[Ca^{2+}]$, CaM_{1234} inhibited IICR. These data clearly show that there is a Ca^{2+}-dependence for the action of CaM, but CaM is not the Ca^{2+} sensor for this Ca^{2+} dependence. Electron microscopy of the IP_3R clearly demonstrated that the conformation of the IP_3R dramatically changes in the presence of Ca^{2+} from a closed to an open "windmill" structure (Hamada et al., 2002, 2003). It is conceivable that CaM tethered to the IP_3R may exert its inhibitory role on the IP_3R only in the open "windmill" configuration.

The functional significance of the CaM-binding site in the regulatory domain still remains an open question. We found that this CaM-binding site seems to be more complex than was described previously (Yamada et al., 1995) and consists of a high-affinity Ca^{2+}/CaM and a lower-affinity apoCaM-binding site (Fig. 3). We can exclude, based on work by Zhang and Joseph (2001) and Nosyreva et al. (2002), the possibility that this site is responsible for the Ca^{2+}-dependent inhibition

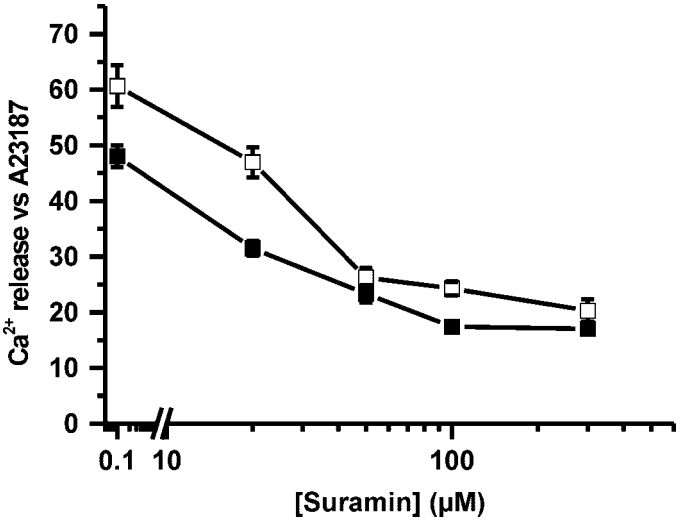

Fig. 6. ATP dependence of the inhibitory effects of suramin on IICR. Ca^{2+} release from permeabilized L15 cells, loaded with $^{45}Ca^{2+}$ during 45 min, was measured after stimulating the cells with 200 nM IP_3. Ca^{2+} release was plotted as a function of increasing concentration of suramin in the presence (□) or absence (■) of 1 mM ATP. Ca^{2+} release was always plotted as the percentage of the maximal releasable fraction by 5 μM A23187. Results represent the means ± S.E. of three independent experiments, each performed twice.

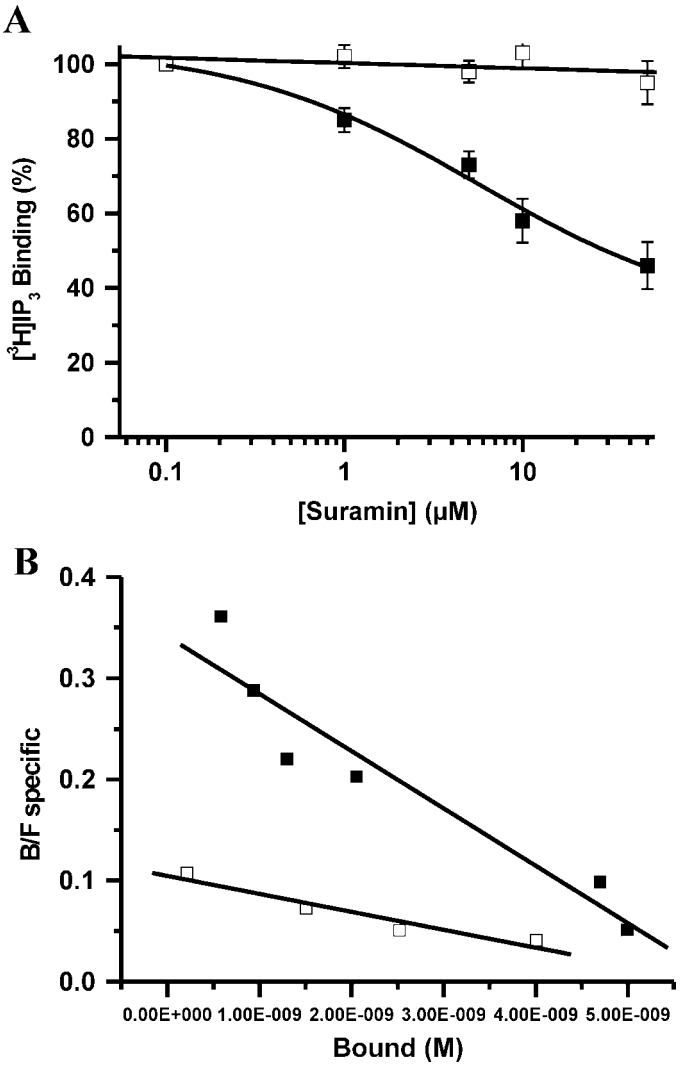

Fig. 7. Effect of suramin on $[^3H]IP_3$ binding to Lbs1 and Lbs1 Δ1–225. A, $[^3H]IP_3$ binding to purified Lbs1 (■) and Lbs1 Δ1–225 (□) in presence of indicated concentrations of suramin was expressed as the percentage of the binding measured without suramin. Binding was measured at pH 7.0 in the presence of 1 mM EGTA and 3.5 nM $[^3H]IP_3$. B, a Scatchard analysis of $[^3H]IP_3$ binding to Lbs1 in the absence or presence of 10 μM suramin is presented. Affinity-purified Lbs1 (1.25 μg) was incubated with 3.5 nM $[^3H]IP_3$ at pH 7.0 and increasing concentrations of unlabeled IP_3 in the absence (■) or presence (□) of 10 μM suramin. Data are expressed as the means ± S.E.M. of at least three experiments.

of the IP_3R. We cannot, however, exclude the possibility that this CaM-binding site indirectly regulates the IP_3R because previous data have shown that CaM binding may depend on the phosphorylation status of the IP_3R1 (Lin et al., 2000).

On the other hand, the lower-affinity CaM-binding site on the N terminus seems to be involved in the direct regulation of the IP_3R by affecting the sensitivity to IP_3. Our finding that suramin mimicked the inhibitory effect of CaM suggests that the N-terminal CaM-binding site may be a protein-protein interaction site involved in structural intramolecular associations, similar to that proposed for RyRs (Slavik et al., 1997; Sencer et al., 2001). The inhibitory effect of both suramin and CaM may then result from a disruption of such an intramolecular interaction. The Ca^{2+} dependence of the inhibition would suggest that this intramolecular interaction is stabilized in the "windmill" configuration of the IP_3R. We cannot exclude, however, the possibility that suramin may inhibit IICR by removing endogenously bound CaM from an as-yet unidentified high-affinity site (Lin et al., 2000). Other members of the CaM family, such as Ca^{2+}-binding proteins (CaBPs), were also shown to interact with the N-terminal part of all IP_3Rs and thereby inhibited IP_3R function (Haynes et al., 2004; Nadif Kasri et al., 2004). There was evidence that CaBP1 interacted at the same binding site as CaM and CaM_{1234} (Nadif Kasri et al., 2004). In another report, however, it was claimed that CaBP1 was an activator of the IP_3R by interaction with the N-terminal part of the IP_3R (Yang et al., 2002). From the present data, we conclude that CaBP1 inhibited IICR in essentially the same way as CaM or CaM_{1234}.

Taken together, our data show that suramin is a potent inhibitor of the IP_3R. It mimicked the effect of CaM, CaM_{1234}, and CaBP1 by inducing an allosteric but competitive inhibition of IP_3-binding. The inhibition of IP_3 binding via the N-terminal CaM-binding site also resulted in lower IP_3 sensitivity for IICR. However, CaM and CaM_{1234} only inhibited IICR in the presence of Ca^{2+}, which indicates that a Ca^{2+}-dependent conformational change is required, but CaM is not the Ca^{2+} sensor for this change.

Further mutational analysis of the N-terminal CaM-binding site should reveal its potential role in the intramolecular interactions required for linking IP_3 binding to IICR.

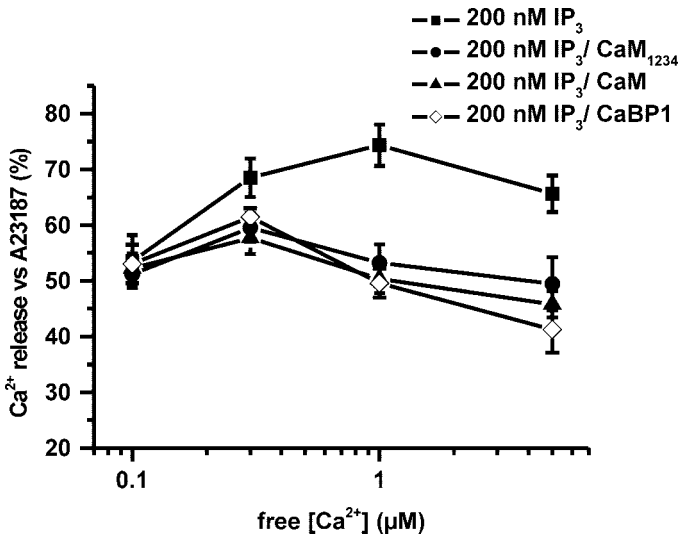

Fig. 8. Effects of CaM, CaM_{1234}, and CaBP1 on IICR in permeabilized L15 cells. Ca^{2+} release from permeabilized L15 cells, loaded with $^{45}Ca^{2+}$ during 45 min, was measured after stimulating the cells with 200 nM IP_3. Ca^{2+} release was plotted as a function of the free $[Ca^{2+}]$ (■). The effects of CaM (▲), CaM_{1234} (●), and CaBP1 (◇) were measured by adding 10 μM concentrations of CaM, CaM_{1234}, or CaBP1, respectively, during the IP_3-induced Ca^{2+} release. Ca^{2+} release was always plotted as the percentage of the maximal releasable fraction by 5 μM A23187. Results represent the means ± S.E. of three independent experiments each performed twice.

Acknowledgments

We thank Lea Bauwens, Marina Crabbé, Silvie De Swaef, and Silvia Vangeel for their technical assistance. The mammalian CaM cDNA was kindly provided by Dr. Z. Grabarek (Boston, MA) and the rat cDNA for CaM_{1234} was kindly provided by Dr. J. Adelman (Portland, OR).

References

Adkins CE, Morris SA, De Smedt H, Sienaert I, Torok K, and Taylor CW (2000) Ca^{2+}-calmodulin inhibits Ca^{2+} release mediated by type-1, -2 and -3 inositol trisphosphate receptors. *Biochem J* **345:**357–363.

Emmick JT, Kwon S, Bidasee KR, Besch KT, and Besch HR (1994) Dual effect of suramin on calcium fluxes across sarcoplasmic reticulum vesicle membranes. *J Pharmacol Exp Ther* **269:**717–724.

Fabiato A and Fabiato F (1979) Calculator programs for computing the composition of the solutions containing multiple metals and ligands used for experiments in skinned muscle cells. *J Physiol* **75:**463–505.

Hamada K, Miyata T, Mayanagi K, Hirota J, and Mikoshiba K (2002) Two-state conformational changes in inositol 1,4,5-trisphosphate receptor regulated by calcium. *J Biol Chem* **277:**21115–21118.

Hamada K, Terauchi A, and Mikoshiba K (2003) Three-dimensional rearrangements within inositol 1,4,5-trisphosphate receptor by calcium. *J Biol Chem* **278:**52881–52889.

Haynes LP, Tepikin AV, and Burgoyne RD (2004) Calcium-binding protein 1 is an inhibitor of agonist-evoked, inositol 1,4,5-trisphosphate-mediated calcium signaling. *J Biol Chem* **279:**547–555.

Islam MO, Yoshida Y, Koga T, Kojima M, Kangawa K, and Imai S (1996) Isolation and characterization of vascular smooth muscle inositol 1,4,5-trisphosphate receptor. *Biochem J* **316:**295–302.

Jurado LA, Chockalingam PS, and Jarrett HW (1999) Apocalmodulin. *Physiol Rev* **79:**661–682.

Khodakhah K and Ogden D (1993) Functional heterogeneity of calcium release by inositol trisphosphate in single Purkinje neurones, cultured cerebellar astrocytes and peripheral tissues. *Proc Natl Acad Sci USA* **90:**4976–4980.

Klinger M, Bofill-Cardona E, Mayer B, Nanoff C, Freissmuth M and Hohenegger M (2001) Suramin and the suramin analogue NF307 discriminate among calmodulin-binding sites. *Biochem J* **355:**827–833.

Laemmli UK (1970) Cleavage of structural proteins during the assembly of the head of bacteriophage T4. *Nature (Lond)* **227:**680–685.

Lin C, Widjaja J, and Joseph SK (2000) The interaction of calmodulin with alternatively spliced isoforms of the type-I inositol trisphosphate receptor. *J Biol Chem* **275:**2305–2311.

Mackrill JJ, Wilcox RA, Miyawaki A, Mikoshiba K, Nahorski SR, and Challiss RA (1996) Stable overexpression of the type-1 inositol 1,4,5-trisphosphate receptor in L fibroblasts: subcellular distribution and functional consequences. *Biochem J* **318:**871–878.

Maes K, Missiaen L, De Smet P, Vanlingen S, Callewaert G, Parys JB and De Smedt H (2000) Differential modulation of inositol 1,4,5-trisphosphate receptor type 1 and type 3 by ATP. *Cell Calcium* **27:**257–267.

Maes K, Missiaen L, Parys JB, De Smet P, Sienaert I, Waelkens E, Callewaert G, and De Smedt H (2001) Mapping of the ATP-binding sites on inositol 1,4,5-trisphosphate receptor type 1 and type 3 homotetramers by controlled proteolysis and photoaffinity labeling. *J Biol Chem* **276:**3492–3497.

Michikawa T, Hirota J, Kawano S, Hiraoka M, Yamada M, Furuichi T, and Mikoshiba K (1999) Calmodulin mediates calcium-dependent inactivation of the cerebellar type 1 inositol 1,4,5-trisphosphate receptor. *Neuron* **23:**799–808.

Missiaen L, Parys JB, Weidema AF, Sipma H, Vanlingen S, De Smet P, Callewaert G, and De Smedt H (1999) The bell-shaped Ca^{2+} dependence of the inositol 1,4,5-trisphosphate-induced Ca^{2+} release is modulated by Ca^{2+}/calmodulin. *J Biol Chem* **274:**13748–13751.

Miyakawa T, Maeda A, Yamazawa T, Hirose K, Kurosaki T, and Iino M (1999) Encoding of Ca^{2+} signals by differential expression of IP3 receptor subtypes. *EMBO (Eur Mol Biol Organ) J* **18:**1303–1308.

Miyakawa T, Mizushima A, Hirose K, Yamazawa T, Bezprozvanny I, Kurosaki T, and Iino M (2001) Ca^{2+}-sensor region of IP_3 receptor controls intracellular Ca^{2+} signaling. *EMBO (Eur Mol Biol Organ) J* **20:**1674–1680.

Miyawaki A, Furuichi T, Maeda N, and Mikoshiba K (1990) Expressed cerebellar-type inositol 1,4,5-trisphosphate receptor, P400, has calcium release activity in a fibroblast L cell line. *Neuron* **5:**11–18.

Nadif Kasri N, Bultynck G, Sienaert I, Callewaert G, Erneux C, Missiaen L, Parys JB, and De Smedt H (2002) The role of calmodulin for inositol 1,4,5-trisphosphate receptor function. *Biochim Biophys Acta* **1600:**19–31.

Nadif Kasri N, Holmes AM, Bultynck G, Parys JB, Bootman MD, Rietdorf K, Missiaen L, McDonald F, Smedt HD, Conway SJ, et al. (2004) Regulation of $InsP_3$ receptor activity by neuronal Ca^{2+}-binding proteins. *EMBO (Eur Mol Biol Organ) J* **23:**312–321.

Nadif Kasri N, Sienaert I, Parys JB, Callewaert G, Missiaen L, Jeromin A and De Smedt H (2003) A novel Ca^{2+}-induced Ca^{2+}-release mechanism in A7r5 cells regulated by calmodulin-like proteins. *J Biol Chem* **278:**27548–27555.

Nosyreva E, Miyakawa T, Wang Z, Glouchankova L, Mizushima A, Iino M and Bezprozvanny I (2002) The high affinity calcium-calmodulin-binding site does not play a role in modulation of type 1 inositol (1,4,5)-trisphosphate receptor function by calcium and calmodulin. *Biochem J* **365:**659–667.

Papineni RV, O'Connell KM, Zhang H, Dirksen RT and Hamilton SL (2002) Suramin interacts with the calmodulin binding site on the ryanodine receptor, RYR1. *J Biol Chem* **277:**49167–49174.

Patel S, Morris SA, Adkins CE, O' Beirne G and Taylor CW (1997) Ca^{2+}-independent inhibition of inositol trisphosphate receptors by calmodulin: redistribution of calmodulin as a possible means of regulating Ca^{2+} mobilization. *Proc Natl Acad Sci USA* **94:**11627–11632.

Rhoads AR and Friedberg F (1997) Sequence motifs for calmodulin recognition. *FASEB J* **11:**331–340.

Sencer S, Papineni RV, Halling DB, Pate P, Krol J, Zhang JZ, and Hamilton SL (2001) Coupling of RYR1 and L-type calcium channels via calmodulin binding domains. *J Biol Chem* **276:**38237–38241.

Sienaert I, Nadif Kasri N, Vanlingen S, Parys JB, Callewaert G, Missiaen L, and De Smedt H (2002) Localization and function of a calmodulin-apocalmodulin-binding domain in the N-terminal part of the type 1 inositol 1,4,5-trisphosphate receptor. *Biochem J* **365:**269–277.

Sipma H, De Smet P, Sienaert I, Vanlingen S, Missiaen L, Parys JB and De Smedt H (1999) Modulation of inositol 1,4,5-trisphosphate binding to the recombinant ligand-binding site of the type-1 inositol 1,4, 5-trisphosphate receptor by Ca^{2+} and calmodulin. *J Biol Chem* **274:**12157–12162.

Slavik KJ, Wang JP, Aghdasi B, Zhang JZ, Mandel F, Malouf N, and Hamilton SL (1997) A carboxy-terminal peptide of the alpha 1-subunit of the dihydropyridine receptor inhibits Ca^{2+}-release channels. *Am J Phys* **272:**1475–1481.

Sugawara H, Kurosaki M, Takata M, and Kurosaki T (1997) Genetic evidence for involvement of type 1, type 2 and type 3 inositol 1,4,5-trisphosphate receptors in signal transduction through the B-cell antigen receptor. *EMBO (Eur Mol Biol Organ) J* **16:**3078–3088.

Taylor CW and Laude AJ (2002) IP3 receptors and their regulation by calmodulin and cytosolic Ca^{2+}. *Cell Calcium* **32:**321–334.

Vanlingen S, Sipma H, De Smet P, Callewaert G, Missiaen L, De Smedt H, and Parys JB (2000) Ca^{2+} and calmodulin differentially modulate myo-inositol 1,4,5-trisphosphate (IP_3)-binding to the recombinant ligand-binding domains of the various IP3 receptor isoforms. *Biochem J* **346:**275–280.

Yamada M, Miyawaki A, Saito K, Nakajima T, Yamamoto-Hino M, Ryo Y, Furuichi T, and Mikoshiba K (1995) The calmodulin-binding domain in the mouse type 1 inositol 1,4,5-trisphosphate receptor. *Biochem J* **308:**83–88.

Yang J, McBride S, Mak DO, Vardi N, Palczewski K, Haeseleer F, and Foskett JK (2002) Identification of a family of calcium sensors as protein ligands of inositol trisphosphate receptor Ca^{2+} release channels. *Proc Natl Acad Sci USA* **99:**7711–7716.

Yoneshima H, Miyawaki A, Michikawa T, Furuichi T, and Mikoshiba K (1997) Ca^{2+} differentially regulates the ligand-affinity states of type 1 and type 3 inositol 1,4,5-trisphosphate receptors. *Biochem J* **322:**591–596.

Zhang X and Joseph SK (2001) Effect of mutation of a calmodulin binding site on Ca^{2+} regulation of inositol trisphosphate receptors. *Biochem J* **360:**395–400.

Address correspondence to: Humbert De Smedt, Laboratorium voor Fysiologie, K. U. Leuven Campus Gasthuisberg O/N, Herestraat 49, B-3000, Leuven, Belgium. E-mail: humbert.desmedt@med.kuleuven.ac.be